Initial ciliary assembly in *Chlamydomonas* requires Arp2/3 complex-dependent endocytosis

Brae M Bigge[1,2], Nicholas E Rosenthal[1,2], Prachee Avasthi[1,2]

[1]Biochemistry and Cell Biology Department, Geisel School of Medicine at Dartmouth College, Hanover, New Hampshire
[2]Anatomy and Cell Biology Department, University of Kansas Medical Center, Kansas City, Kansas

ABSTRACT

Ciliary assembly, trafficking, and regulation are dependent on microtubules, but the mechanisms of ciliary assembly also require the actin cytoskeleton. Here, we dissect subcellular roles of actin in ciliogenesis by focusing on actin networks nucleated by the Arp2/3 complex in the powerful ciliary model, *Chlamydomonas*. We find the Arp2/3 complex is required for the initial stages of ciliary assembly when protein and membrane are in high demand, but cannot yet be supplied from the Golgi complex. We provide evidence for Arp2/3 complex-dependent clathrin-mediated endocytosis of ciliary proteins, an increase in endocytic activity upon induction of ciliary growth, and relocalization of plasma membrane proteins to newly formed cilia. Our data support a new model of ciliary protein and membrane trafficking during early ciliogenesis whereby proteins previously targeted to the plasma membrane are reclaimed by Arp2/3 complex-dependent clathrin-mediated endocytosis for initial ciliary assembly.

INTRODUCTION

The cilium of the unicellular, green alga *Chlamydomonas reinhardtii* has long been used as a model due to its structural and mechanistic conservation relative to the cilia of mammalian cells. Cilia consist primarily of microtubules that extend from the surface of the cell and are ensheathed in plasma membrane. Their assembly relies on microtubule dynamics and trafficking of protein and membrane (Nachury, Seeley, and Jin 2010), as well as intraflagellar transport (IFT), a motor-based transport system that moves tubulin and other cargo from the base of the cilium to the tip and back again (Pedersen and Rosenbaum 2008).

Although cilia are composed of microtubules and depend on them for assembly, the mechanisms governing ciliary maintenance and assembly extend to other cytoskeletal components, such as actin. In mammalian cells, actin disruption results in increased ciliary length and percentage of ciliated cells (Kim et al. 2010; Park et al. 2008). In fact, the microtubule organizing center of the cell, the centrosome, from which cilia are nucleated has been found to function as an actin organizer (Farina et al. 2016; Inoue et al. 2019). Further, in mammalian cells, when ciliogenesis is triggered by serum starvation, preciliary vesicles are trafficked to the centriole where they fuse to form a ciliary vesicle around the budding cilium. In the intracellular pathway of ciliogenesis, it has been shown that when Arp2/3 complex-branched actin is lost, depletion of preciliary vesicles at the centriole occurs due to problems with vesicle fusion, suggesting a role for branched actin in intracellular ciliogenesis (Wu, Chen, and Tang 2018). Further, actin itself has even been found within cilia, suggesting that actin is a key protein involved in ciliary maintenance and assembly (Kiesel et al. 2020).

Chlamydomonas cells are ideal for tackling the question of actin-dependent ciliary trafficking due to their lack of a cortical actin network and their ability to undergo more consistent and robust ciliogenesis than mammalian cells without requiring serum starvation. In *Chlamydomonas*, disruption of actin networks with Cytochalasin D (CytoD) resulted in shorter steady-state cilia (W. L. Dentler and Adams 1992) and disruption with Latrunculin B (LatB), which sequesters monomers leading to eventual filament depolymerization, resulted in shortened cilia and impaired regeneration (Avasthi et al. 2014; Jack et al. 2019). *Chlamydomonas* actin networks are required for accumulation of IFT machinery at the base of cilia and for entry of IFT material into cilia (Avasthi et al. 2014), as well as for trafficking of post-Golgi vesicles to cilia, the synthesis of ciliary proteins, and the organization of the gating region at the base of cilia (Jack et al. 2019). Many key advances in our understanding of the relationship between cilia and actin have been discovered using *Chlamydomonas*, which is proving to be a useful model for studying the actin cytoskeleton and its ciliary functions.

The actin cytoskeleton of *Chlamydomonas* contains two actin genes: *IDA5*, a conventional actin with 91% sequence identity to human β-actin; and *NAP1*, a divergent actin that shares only 63% of its sequence with human β-actin (Hirono et al. 2003; Kato-Minoura et al. 1998). We consider NAP1 to be an actin-like protein as opposed to an actin related protein (ARP) because it has a higher sequency identity to actin than to conventional ARPs, and because it is able to functionally compensate for the conventional filamentous actin (Jack et al. 2019; M. Onishi et al. 2018; M. Onishi, Pringle, and Cross 2016; Masayuki Onishi et al. 2019). Under normal, vegetative conditions, the conventional IDA5 is the primary actin expressed, but when cells are treated with LatB, the LatB-insensitive NAP1 is upregulated (M. Onishi et al. 2018; M. Onishi, Pringle, and Cross 2016; Hirono et al. 2003). This separability of the two actins has led to the discovery that they can compensate for each other in ciliary maintenance and assembly (Jack et al. 2019). Studies of the role of actin in ciliary assembly have used global disruption by knocking out either one of the filamentous actins or acutely both, yet actin networks have diverse compositions and topologies that lead to specific subfunctions within cells.

Actin networks rely on the actin binding proteins that contribute to the formation, arrangement, and function of the network. One such actin binding protein is the Arp2/3 complex,

which nucleates branched or dendritic actin networks by nucleating a daughter filament off the side of an existing mother filament. The dendritic networks nucleated by the Arp2/3 complex have been primarily found to be responsible for functions that involve membrane remodeling, for example lamellipodia and endocytosis (Campellone and Welch 2010). The Arp2/3 complex from most eukaryotes consists of seven subunits: Arp2, Arp3, and ARPC1-5 (**Supplemental Figure 1**) and each subunit plays a specific role of varying importance in the nucleation process. ARPC2 and ARPC4 form the core of the complex and the primary contacts with the mother filament, Arp2 and Arp3 serve as the first subunits of the daughter filament, and ARPC1 and ARPC3 play a role in nucleation but are not critical for branch formation (Robinson et al. 2001; Gournier et al. 2001). Each of these subunits are found in *Chlamydomonas* but have varying degrees of sequence homology compared with conventional Arp2/3 complexes (**Supplemental Figure 1**). Interestingly, the ARPC5 subunit has yet to be found in *Chlamydomonas*. ARPC5 is thought to be important for the association of ARPC1 to the complex, but a mammalian complex lacking ARPC5 and ARPC1 maintains some nucleating and branching activity and is able to cross-link actin normally (Gournier et al. 2001).

Here, using the chemical inhibitor CK-666 to inhibit the nucleating function of the Arp2/3 complex (Hetrick et al. 2013) and a genetic mutant of a critical Arp2/3 complex member, ARPC4 (Cheng et al. 2017; Li et al. 2019), we take a more delicate approach to investigating the role of actin in ciliary assembly by separating different actin networks into their subfunctions based on topology. Specifically, we probe the involvement of actin networks nucleated by the Arp2/3 complex in ciliary maintenance and assembly. This approach in these cells has allowed us to propose a new model implicating a subset of filamentous actin in redistribution of membrane and proteins for the initial stages of ciliogenesis.

RESULTS

Loss of Arp2/3 complex function inhibits normal regeneration and maintenance of cilia:

We first investigated the requirement for the Arp2/3 complex in maintenance of cilia by treating cells with varying concentrations of CK-666, the inhibitor of the Arp2/3 complex, or the inactive control CK-689 (250μM) for 2 hours and measuring the effect on steady state ciliary length. Consistent with previous results (Avasthi et al. 2014), we found that treating cells with CK-666 decreased ciliary length, suggesting that the Arp2/3 complex is required for maintaining cilia (**Figure 1A**). We saw no changes in ciliary length with the inactive CK-689 (**Figure 1A**) or when *arpc4* mutant cells lacking a functional Arp2/3 complex were treated with CK-666 (**Supplemental Figure 2**). Untreated *arpc4* mutant cells recapitulate the CK-666 result and have a decreased ciliary length when compared with wild-type cells (**Figure 1B**) demonstrating through both chemical and genetic perturbation that the Arp2/3 complex is required for normal ciliary length maintenance.

Next, we probed the involvement of Arp2/3 complex-nucleated actin in the more complicated process of ciliary assembly where there is a high demand for protein and membrane both from pools already existing in the cell and from synthesis (Wingfield et al. 2017; Nachury, Seeley, and Jin 2010; Rohatgi and Snell 2010; Jack et al. 2019; Diener, Lupetti, and Rosenbaum 2015). Cells were deciliated by low pH shock and then allowed to synchronously regenerate cilia after being returned to normal pH (Paul A. Lefebvre 1995). We found that cells lacking a functional Arp2/3 complex were slow to regenerate their cilia, and two-thirds of cells did not regrow cilia at all (**Figure 1C**). Importantly, the initial steps are the slowest portion of assembly when existing protein and membrane are being incorporated into cilia.

This result is puzzling because the loss of Arp2/3 complex function, and therefore only a subset of actin filaments, results in a more dramatic phenotype than that of the *nap1* mutants treated with LatB, which are lacking all filamentous actins (Jack et al. 2019). However, in the

126 *arpc4* mutant cells, a functional Arp2/3 complex never exists, and therefore, cells never have
127 Arp2/3 complex-mediated actin networks. In *nap1* mutant cells treated with LatB, the treatment
128 begins shortly after deciliation causing an acute perturbation. Further, LatB functions by
129 sequestering actin monomers to promote filament disassembly, and thus the effects may not be
130 immediate (Spector et al. 1989). Therefore, it is likely that there is a brief window where actin
131 filaments can assert their initial role in ciliary regeneration before being depolymerized. To avoid
132 this, we began the LatB treatment in *nap1* mutants 30 minutes before deciliation. This pre-
133 treatment allows us to observe what happens when actin is not present immediately after
134 deciliation. (**Figure 1D-E**). In this case, we see decreased ciliary length and dramatically
135 decreased percent ciliation, which is consistent with the *arpc4* mutant results.
136

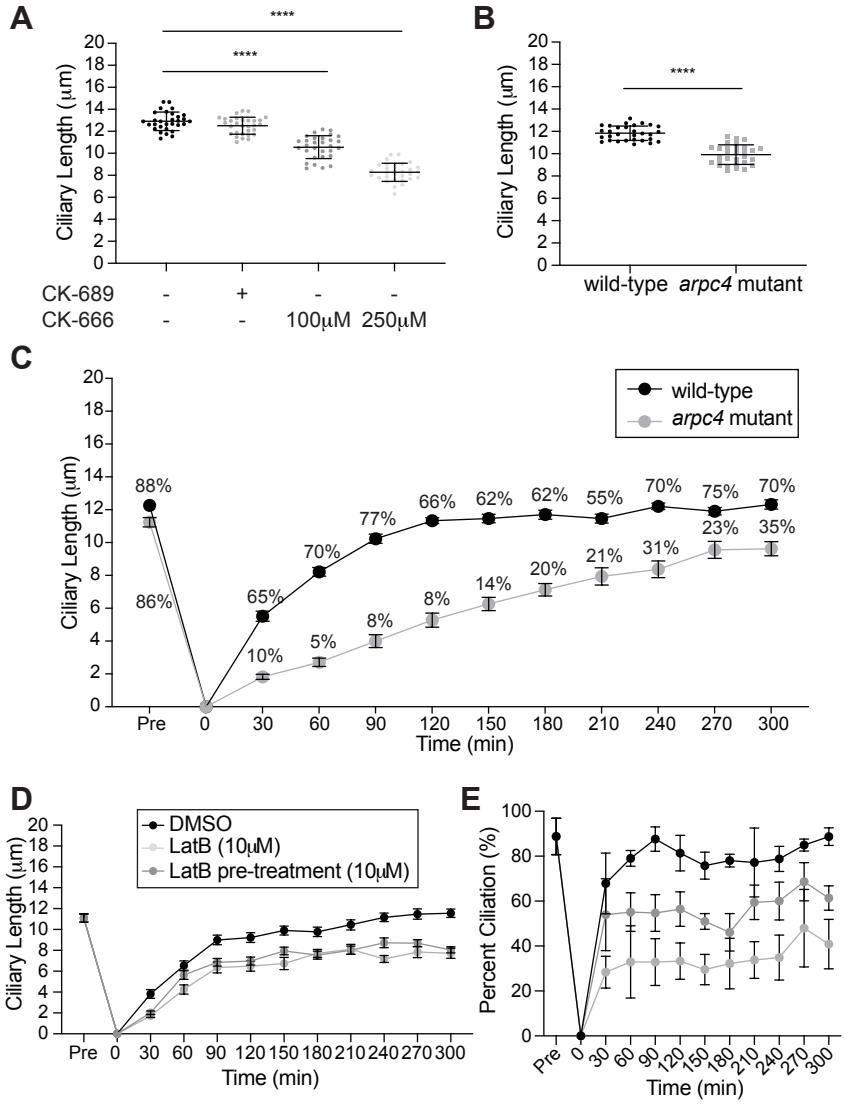

137
138 **Figure 1. The Arp2/3 complex is required for normal ciliary maintenance and assembly. A)** Wild-type cells were
139 treated with 100μM or 250μM CK-666 or the inactive CK-689 for 2 hours. Cells were then imaged using a DIC
140 microscope and cilia were measure in ImageJ. The mean is displayed with error bars representing standard deviation.
141 n=30 for each treatment in 3 separate experiments. P<0.0001. **B)** Wild-type cells and *arpc4* mutant cells steady state
142 cilia were also measured with no treatment. The mean is displayed with error bars representing standard deviation.
143 n=30 for each strain for 3 separate experiments. P<0.0001. **C)** Wild-type cells and *arpc4* mutant cells were deciliated
144 using a pH shock and then allowed to regrow. The black line represents wild-type, while the grey line represents the
145 *arpc4* mutant. The numbers above or below each point show the percent ciliation for the wild-type and *arpc4* mutant

cells respectively. Means are displayed with error bars representing 95% confidence interval. n=30 for each strain and each time point in 3 separate experiments. For every time point except 0 min, P<0.0001 in terms of both length and percent ciliation. **D)** *nap1* mutant cells were pre-treated with 10μM LatB for 30 minutes before deciliation or treated with LatB upon the return to neutral pH following deciliation. The black line represents untreated cells, while the light grey line represents cells treated with LatB following deciliation and the dark grey line represents cells pre-treated with LatB. Error bars represent standard deviation. N=3 separate experiments. For every time point P>0.0001 between DMSO and treated samples, except 30min (10μM LatB) which is ns. Asterisks for the pretreatment are located below the graph, while asterisks for the post treatment are located above the line. **E)** Percent ciliation for the experiment in D. Line color is the same as D. Error bars represent standard deviation.

The Arp2/3 complex is required for the incorporation of existing membrane and proteins for ciliary assembly:

There are several distinct steps of ciliary assembly after severing, all of which require actin filaments. The first step requires that a pool of existing proteins and membrane are incorporated into cilia in an actin-dependent manner (Jack et al. 2019). As disruption of Arp2/3 complex-mediated actin networks results in slow initial ciliary assembly, when it is likely that existing protein is being incorporated, we questioned the involvement of Arp2/3 complex-dependent actin networks in the incorporation of existing ciliary protein.

By treating cells with cycloheximide (CHX), a protein synthesis inhibitor, we can eliminate the contribution of two steps in the process of ciliary assembly (**Figure 2A**) (Rosenbaum, Moulder, and Ringo 1969). Without protein synthesis, there is no trafficking or incorporation of new proteins. Therefore, any ciliary growth we see is due to the incorporation of the existing protein alone. Under normal conditions, cells that are deciliated and treated with cycloheximide typically grow cilia to about half-length, or 6μm, within 2 hours (**Figure 2B**). We also saw cells growing to half-length after 2 hours when treated with the inactive CK-689 and cycloheximide (**Figure 2B**). However, when treated with either 100μM or 250μM CK-666 and cycloheximide, cells exhibit a dose-dependent decrease in ciliary length after 2 hours of regeneration (**Figure 2B**).

To confirm the results of chemical perturbation, we used the *arpc4* mutant strain to genetically test the role of the Arp2/3 complex in incorporation of existing protein. When *arpc4* mutant cells were deciliated and treated with cycloheximide, they display minimal growth (**Figure 2C**). In fact, throughout a five-hour period, only 6% of cells were able to form cilia at all (**Figure 2C**). This suggests that the Arp2/3 complex and the actin networks nucleated by the complex are indispensable for the incorporation of existing protein and membrane during ciliary assembly. This can be further dissected because we know in the case of cells treated with cycloheximide and CK-666, the protein pool is available but is still not incorporated, suggesting a problem with membrane incorporation or delivery as opposed to a problem with protein availability.

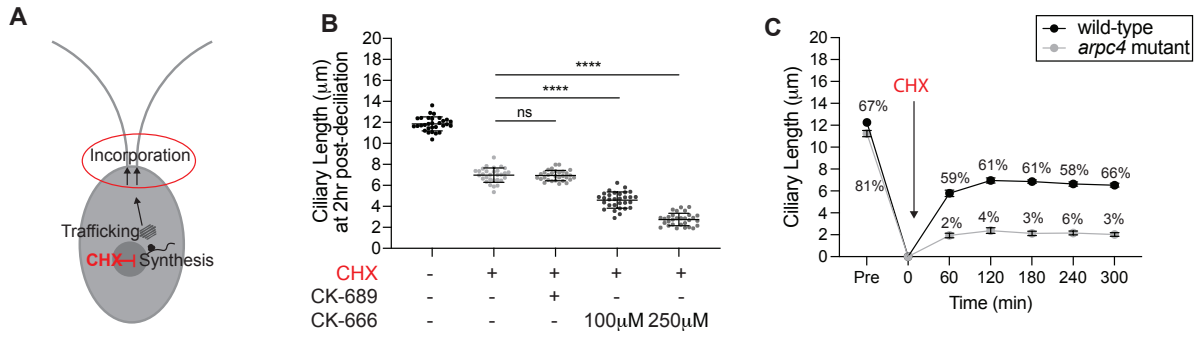

Figure 2. The Arp2/3 complex is required for incorporation of existing protein during ciliary assembly. A) Treating cells with cycloheximide inhibits protein synthesis, which means only incorporation of existing protein into the

cilia is observed**. B)** Wild-type cells were deciliated and then treated with a combination of 10μM cycloheximide (CHX) and CK-666 (100μM or 250μM) or CK-689 (the inactive control) at the same concentration during regrowth. The graph shows the length of their cilia after 2 hours of treatment and regrowth. The mean is show with error bars representing standard deviation. n=30 for each treatment group 3 separate experiments. For both the 100μM and 250μM CK-666 treatments with CHX, P<0.0001. **C)** Wild-type cells and *arpc4* mutants were deciliated and then allowed to regrow in 10μM CHX. The percentages above the lines represent the percent of cells with cilia at the indicated time points. The mean is shown with error bars representing 95% confidence interval. n=30 for each strain and each time point in 3 separate experiments. For every time point besides 0 min, P<0.0001 for both length and percent ciliation.

Cilia of *arpc4* mutant cells resorb faster in the absence of the Golgi:

Because we see defects in ciliary assembly and maintenance when cells are likely incorporating existing protein, and we know the protein needed for assembly is in excess due to our acute perturbations with CK-666, we next investigated membrane delivery to cilia. This is of particular interest as the Arp2/3 complex is canonically thought to be involved in membrane remodeling functions. Typically, the Golgi is known to be the main source of membrane for cilia (Nachury, Seeley, and Jin 2010; Rohatgi and Snell 2010), and both ciliary membrane, membrane proteins, and even axonemal proteins are transported in or attached to vesicles (Wood and Rosenbaum 2014). In *Chlamydomonas*, this has been demonstrated by the ciliary shortening of cells treated with Brefeldin A (BFA), a drug that causes Golgi collapse by interfering with ER to Golgi transport (W. Dentler 2013). To determine if the Arp2/3 complex is involved in the trafficking of new protein from the Golgi to cilia, we examined the Golgi following deciliation using transmission electron microscopy (TEM) in *arpc4* mutants (**Supplemental Figure 3A**). The Golgi appeared grossly normal, and in all cases had approximately the same number of cisternae (**Supplemental Figure 3A-B**) and did not show an abnormal accumulation of post-Golgi membrane as previously reported when perturbing all filamentous actin (Jack et al., 2019).

Alternative pathways for ciliary material have also been found in *Chlamydomonas*. In previous experiments, surface proteins were biotinylated and then cells were deciliated, meaning the membrane and proteins within cilia were lost. When cilia were allowed to regrow, biotinylated proteins were found to reside within the new cilia suggesting they came from the plasma membrane (W. Dentler 2013). Therefore, we hypothesized that due to its role in membrane remodeling, and particularly endocytosis in other organisms, the Arp2/3 complex may be part of an endocytic pathway that provides membranes and perhaps membrane proteins to cilia (**Figure 3A**). To test if membrane could be coming from an endosomal or endocytic source other than the Golgi, we treated cells with 36μM BFA to collapse the Golgi so cells would be forced to utilize other sources of ciliary proteins and membranes. Wild-type cells treated with BFA resorb slowly, but *arpc4* mutant cells had a faster resorption rate (**Figure 3B and D**). Further, the number of cells with cilia in the *arpc4* mutant cells dramatically decreased with BFA treatment (**Figure 3C**). Meanwhile, cells treated with known-ciliary resorption-inducing drugs that don't specifically target Golgi traffic, 3-isobutyl-1-methylxanthine (IBMX) (Pasquale and Goodenough 1987) or sodium pyrophosphate (NaPPi) (P. A. Lefebvre et al. 1978) show an increased velocity of resorption in the wild-type cells compared to the *arpc4* mutant cells (**Supplemental Figure 4**). Thus, wild-type cells are more capable of maintaining cilia without membrane supply from the Golgi, suggesting that there must be another source for membrane that is dependent upon the Arp2/3 complex.

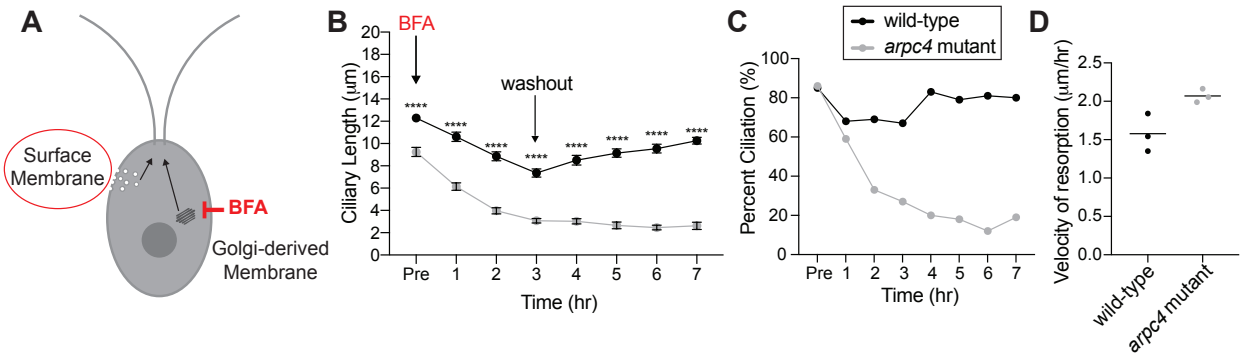

Figure 3. The Arp2/3 complex is required for ciliary maintenance in the absence of intact Golgi. A) Treating cells with BrefeldinA (BFA) causes the Golgi to collapse meaning any membranes and proteins used to maintain the cilia must come from other sources. **B)** Cells were treated with 36µM BFA for 3 hours at which time the drug was washed out. Wild-type is represented by black, while *arpc4* mutants are grey. The mean is shown with error bars representing 95% confidence interval. Error bars represent 95% confidence interval of the mean. n=30 for each time point and each strain in 3 separate experiments. **** represents P<0.0001. **C)** Percent ciliation of the cells in B. n=100. **D)** Resorption speed for wild-type cells and *arpc4* mutant cells as determined by fitting a line to the first 4 time points before washout and determining the slope of the line. Line represents the mean of 3 separate experiments. N=3. P=0.0314

Apical actin dots are dependent on the Arp2/3 complex:

Since ciliary membrane proteins can come from the Golgi or the plasma membrane and *arpc4* mutant cells have a more severe defect in incorporating ciliary proteins from non-Golgi sources, we asked if Arp2/3 complex-mediated actin networks might be responsible for endocytosis from the plasma membrane in *Chlamydomonas* as it is in other organisms. To determine where in the cell Arp2/3 complex-mediated actin networks might be acting, we looked directly at the effects of loss of Arp2/3 complex function on the actin structures in the cell. Using new protocols for the visualization of actin in *Chlamydomonas* developed by our lab (Craig et al. 2019), we stained wild-type cells and *arpc4* null mutant cells with fluorescent phalloidin. In wild-type cells, apical dots reminiscent of endocytic actin patches in yeast are typically seen near the base of cilia (**Figure 4A and A'**). We quantified the presence of these dots in the wild-type cells compared to the *arpc4* mutant cells (**Figure 4B and B'**). We found that while about 70% of wild-type cells contain the dots, only about 5% of the *arpc4* mutant cells had dots (**Figure 4C**), suggesting the Arp2/3 complex is required for the formation of this actin structure. The reliance of this structure on the Arp2/3 complex, led us to further question whether these dots could represent endocytic membrane remodeling.

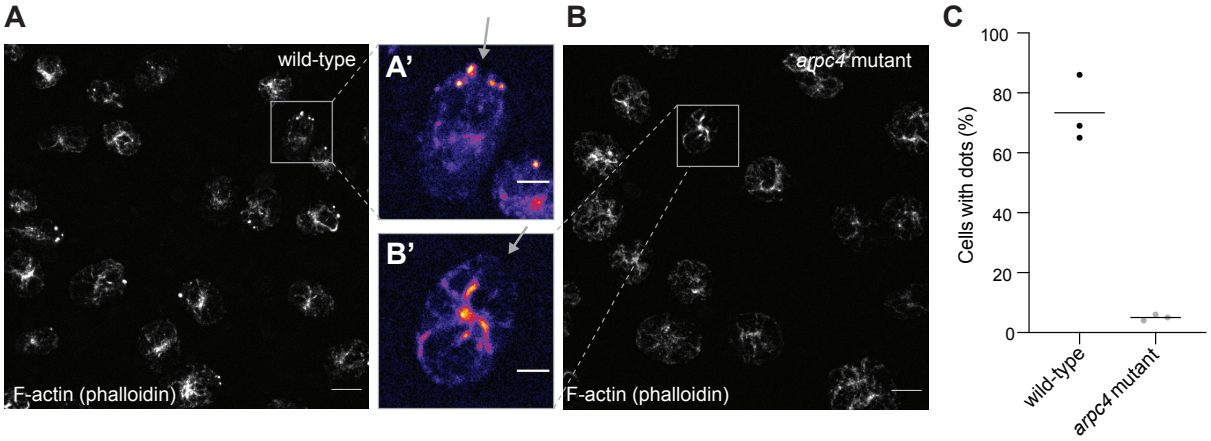

Figure 4. Loss of a functional Arp2/3 complex results in changes in actin distribution. A) Wild-type stained with phalloidin to visualize the actin network. Images were taken as a z-stack using spinning disk confocal imaging and are shown as a maximum intensity projection. Scale bar represents 10μm. A' shows the mid-cell actin network of the wild-type cells. The actin distribution is highlighted using the Fire LUT which highlights regions with the brightest intensity in yellow/orange and the areas with less intensity in blue. Grey arrow is pointing to the apex of the cell. Scale bar represents 2μm. **B)** *arpc4* mutant cells stained with phalloidin to visualize actin. Cells were imaged and are shown in the same way as A. Scale bar represents 10μm. B' shows lack of apical dots and the mid-cell actin staining of *arpc4* mutant cells. Image is shown in the same way as A'. Grey arrow is pointing to the apex of the cell. Scale bar represents 2μm. **C)** Percentage of cells with apical dots as shown in A'. Percentages taken from 3 separate experiments where n=100. Line represents the mean. P<0.0001.

Endocytosis in *Chlamydomonas* is clathrin-dependent:

The Arp2/3 complex is conventionally thought to be involved in endocytosis in cell-walled yeast to overcome turgor pressure (Aghamohammadzadeh and Ayscough 2009; Basu, Munteanu, and Chang 2014; Carlsson and Bayly 2014). *Chlamydomonas* cells also have a cell wall and since the apical actin dots resemble these endocytic pits (Goode, Eskin, and Wendland 2015; Adams and Pringle 1984; Ayscough et al. 1997), we hypothesized that Arp2/3 complex and actin-dependent endocytosis might be occurring in *Chlamydomonas* even though this process has not yet been directly demonstrated in this organism. We compared the endocytosis-related proteins found in mammals and plants to those in *Chlamydomonas* (**Figure 5A**). We found that *Chlamydomonas* was lacking much of the important machinery for almost all typical endocytosis processes, including caveolin for caveolin-mediated endocytosis, flotillin for flotillin-dependent endocytosis, and endophilin for endophilin-dependent endocytosis (**Figure 5A**). However, most of the canonical clathrin-related endocytosis machinery could be found in *Chlamydomonas*, suggesting that clathrin-mediated endocytosis is conserved to a higher extent than other endocytic mechanisms.

We further probed the likelihood of clathrin-mediated endocytosis occurring in *Chlamydomonas* by treating cells with PitStop2 which inhibits the interaction of adaptor proteins with clathrin, halting clathrin-mediated endocytosis itself. The ability of PitStop2-treated cells to internalize membrane was tested using the membrane dye FM 4-46FX, which is usually quickly endocytosed into cells showing bright foci where dye is enriched in endocytosed compartments (**Figure 5B**). We found that cells treated with 30μM PitStop2 have significantly decreased membrane internalization, meaning clathrin is required for the internalization of this membrane dye (**Figure 5C**), which further supports the idea that clathrin-mediated endocytosis is occurring in *Chlamydomonas*.

Finally, we tested whether the endocytosis is Arp2/3 complex-dependent by using this membrane internalization assay on *arpc4* mutant cells compared to wild-type cells. We found that cells lacking a functional Arp2/3 complex have decreased total cell fluorescence (**Figure 5D-E**) suggesting the clathrin-mediated endocytosis in *Chlamydomonas* is Arp2/3 complex-dependent.

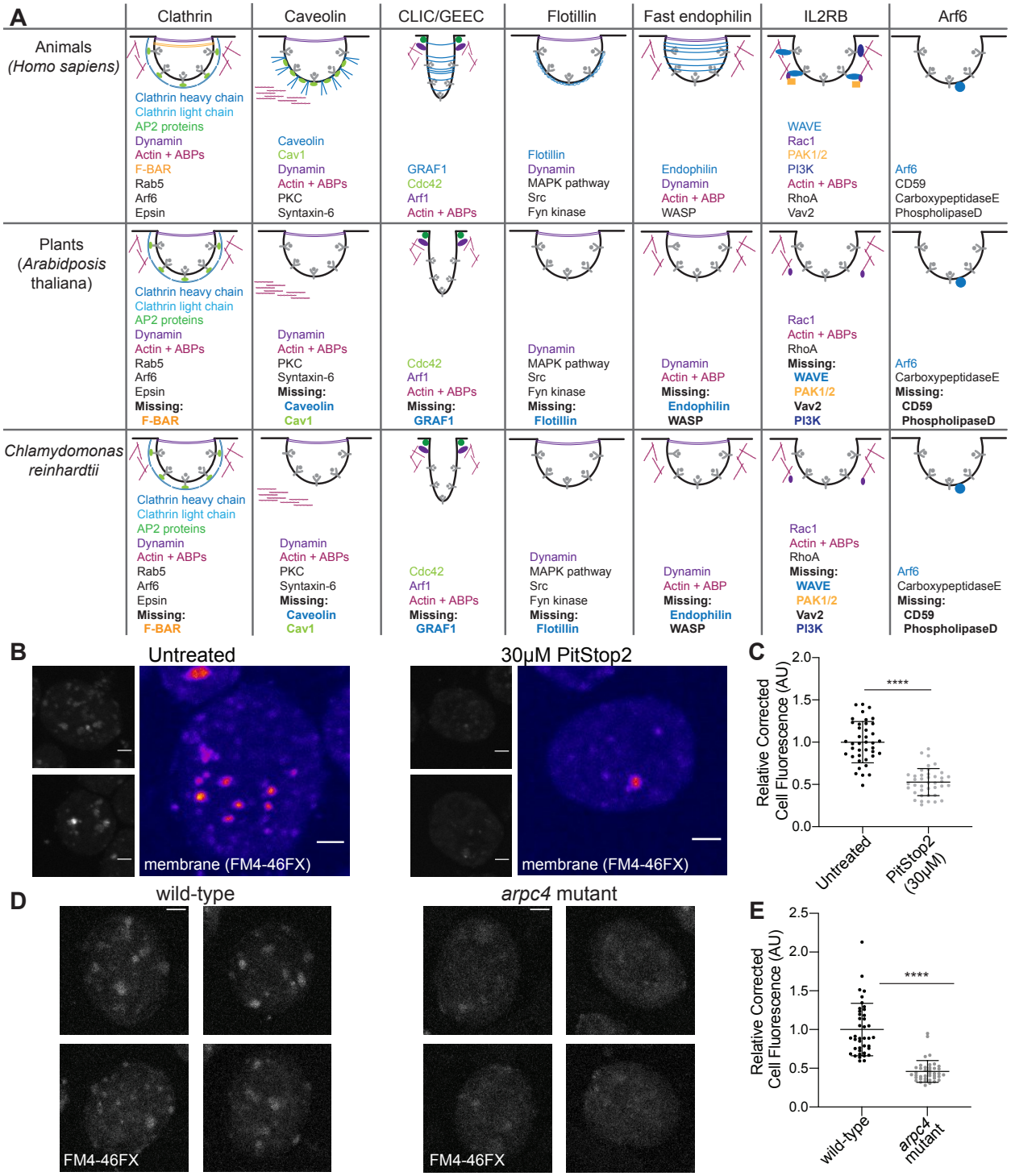

Figure 5. Arp2/3 complex-dependent clathrin-mediated endocytosis is conserved in *Chlamydomonas*. A) Gene presence was determined using BLAST. Word colors correspond to diagram colors. **B)** Cells treated with 30μM PitStop2 were incubated with FM4-46FX and imaged on a spinning disk confocal. Max intensity projections of z-stacks are shown. Scale bars are 2μm. **C)** The background corrected fluorescence for each sample. The mean is shown with error bars showing standard deviation. n=40 in 3 separate experiments. P<0.0001. **D)** Wild-type and *arpc4* mutant cells treated with FM4-46FX and imaged on a spinning disk confocal. Max intensity projections of z-stacks are shown. Scale bars are 2μm. **E)** The background corrected fluorescence for each sample. The mean is shown with error bars representing standard deviation. n=30 in 3 separate experiments. P<0.0001.

318
319 **The Arp2/3 complex is required for the internalization and relocalization of a membrane**
320 **protein from the periphery of the cell to cilia:**
321 Upon finding that there is likely Arp2/3 complex-dependent clathrin-mediated
322 endocytosis in *Chlamydomonas*, we next asked if this endocytosis could be responsible for the
323 relocalization and internalization of a known ciliary protein. SAG1 is a membrane protein that
324 relocalizes to cilia and is important for helping cells stick together or agglutinate in mating
325 *Chlamydomonas* cells (Belzile et al. 2013). When cells are induced for mating with dibutyryl-
326 cAMP (db-cAMP), SAG1 must relocalize from the cell periphery to cilia, where it facilitates ciliary
327 adhesion between mating cells. This relocalizaiton of SAG1 is thought to occur through
328 internalization of the protein followed by internal trafficking on microtubules to the base of cilia
329 (Belzile et al. 2013).
330 We examined whether actin and the Arp2/3 complex were required for the transport of
331 HA-tagged SAG1 to the apex of the cell and cilia for agglutination during mating (**Figure 6A**).
332 Using immunofluorescence, we observed cells treated with either 10μM LatB to depolymerize
333 IDA5 or 250μM CK-666 to perturb the Arp2/3 complex. Before induction, SAG1-HA localized to
334 the periphery of the cell (**Figure 6B, top**). 30 minutes after induction with db-cAMP, SAG1-HA
335 relocalized to the apex of the cell and to cilia in untreated cells (**Figure 6B, left**). In both LatB
336 and CK-666 treated cells, this apical enrichment was greatly decreased (**Figure 6B, middle**
337 **and right**). To quantify this, line scans were drawn through the cell from the apex to the basal
338 region (**Figure 6C-D**). The percentage of cells with apical enrichment was calculated, and it was
339 found that untreated cells had a higher percent of apical enrichment when compared with LatB
340 or CK-666 treated cells (**Figure 6E**). Thus, cells with perturbed Arp2/3 complex-mediated
341 filamentous actin show decreased efficiency of SAG1-HA relocalization.
342 We next asked if this decrease in relocalization in cells with actin and Arp2/3 complex
343 inhibition could be due to a decrease in the internalization of SAG1-HA through a process that
344 seems to require endocytosis. In order to investigate this, we used a method first described by
345 Belzile et al. 2013, where cells were induced and treated with a low percentage (0.01%) of
346 trypsin which will hydrolyze exterior proteins but cannot enter the cell. This assay allows us to
347 determine the efficiency of internalization of SAG1-HA. In untreated cells, we see an increase in
348 SAG1-HA protein levels following induction because SAG1-HA is internalized and becomes
349 protected from trypsin (**Figure 6F**). In cells treated with either 10μM LatB or 250μM CK-666 we
350 see a decrease in this trypsin protection as shown in the western blot (**Figure 6F**). This was
351 further quantified by subtracting the amount of protein before induction from the amount of
352 protein present after induction. This gives a value representing the amount of SAG1-HA
353 protected from trypsin due to induction in these cells (**Figure 6G**). The decrease in SAG1-HA
354 following induction in cells with decreased filamentous actin and Arp2/3 complex function
355 indicates a role for Arp2/3 complex-mediated actin networks in internalization of this ciliary
356 protein.
357

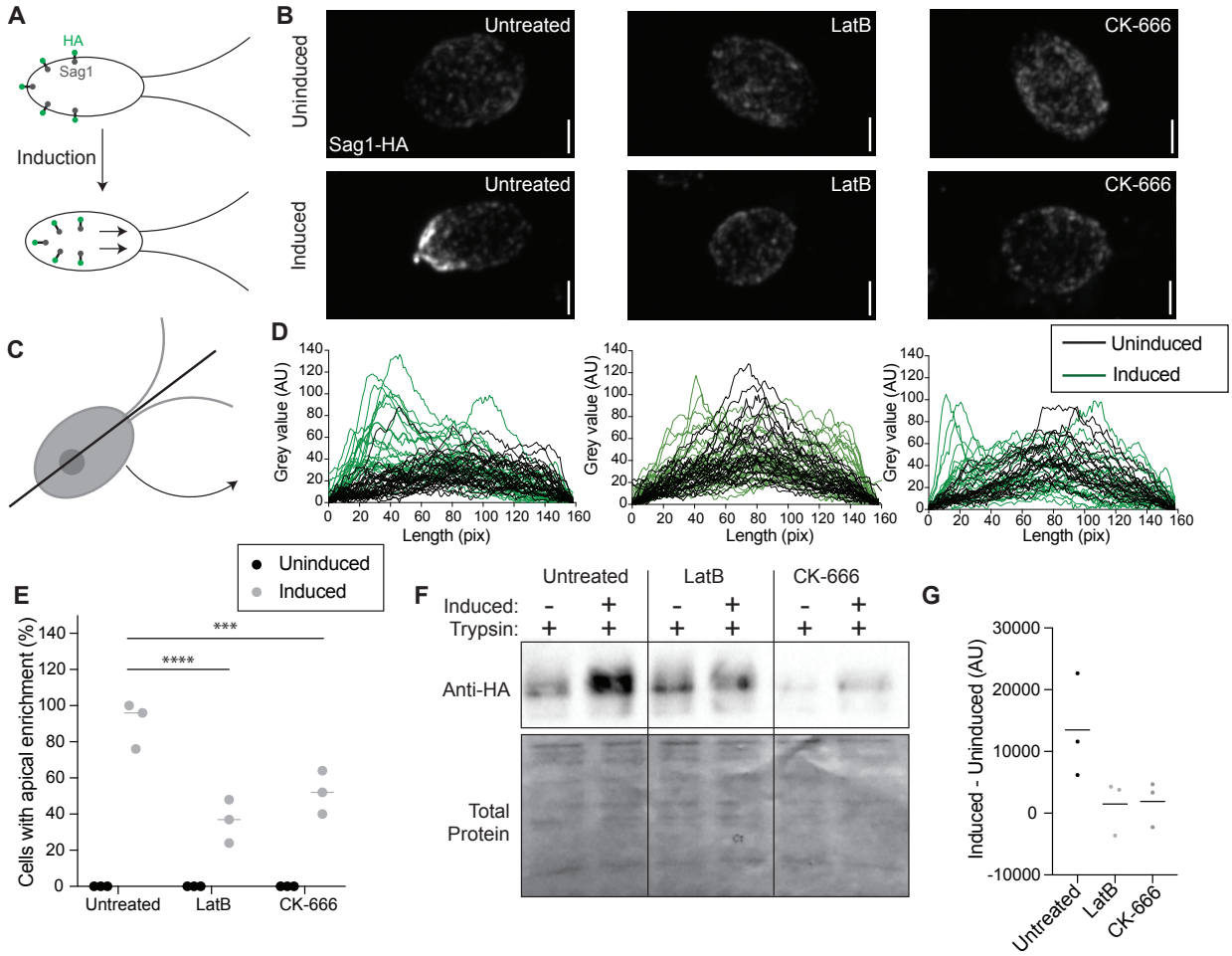

Figure 6. The Arp2/3 complex is required for the relocalization and internalization of the ciliary protein SAG1 for mating. A) When mating is induced SAG1-HA is internalized and relocalized to the apex of the cells and cilia for agglutination. **B)** Maximum intensity projections of z-stacks taken using spinning disk confocal microscopy of SAG1-HA. Left is untreated, middle is treated with 10μM LatB, and right is treated with 250μM CK-666. Top row of images are uninduced and bottom row of images are induced with db-cAMP. Scale bar represents 2μm. **C)** Diagram representing line scans taken through the cells in z-stack sum images. **D)** Line scans from the apex of the cell to the basal region of the cell in untreated cells (left), LatB treated cells (middle), and CK-666 (right). Black lines represent uninduced samples, green lines represent induced samples. **E)** Percentage of cells with apical enrichment based on E for uninduced (black) and induced (grey) cells for each treatment group. The mean is shown with error bars representing standard deviation. n=30 for 3 separate experiments for each treatment. **F)** Western blot showing amount of SAG1-HA in uninduced and induced cells in each treatment group all treated with 0.01% trypsin. **G)** Intensity of the bands in H were normalized to the total protein as determined by amido black staining and quantified in ImageJ was used to subtract uninduced from induced to give a representation of the amount of SAG1-HA internalized with induction. Line represents mean of 3 separate experiments.

Actin dots increase in an Arp2/3 complex and clathrin-dependent manner following deciliation:

Having established that the Arp2/3 complex is required for ciliary assembly, the endocytosis of a known ciliary protein, and membrane dye internalization, we wondered if these functions could be connected given that *arpc4* mutant cells have defects in maintaining cilia from non-Golgi sources (**Figure 3**). Therefore, we returned to the clathrin and Arp2/3 complex-dependent actin dots seen in wild-type cells that are reminiscent of endocytic pits in yeast. Because ciliary membrane and proteins can come from the plasma membrane (Dentler, 2013),

we suspected there would be an increase in these actin dots immediately following deciliation. We used phalloidin to visualize the actin cytoskeleton of wild-type cells before and immediately following deciliation, as well as 10 minutes later (**Figure 7A**). We saw an increase in both the percentage of cells with dots and the number of dots per cell immediately following deciliation that then returned to normal by 10 minutes (**Figure 7A-B**). Importantly, this is consistent with the results shown in **Figure 1D-E** and confirms that the defect seen in ciliary assembly is due to an event occurring very early in ciliary assembly, even within the first few minutes after deciliation.

We wondered if this increase in dots was really due to clathrin-mediated endocytosis, so we treated cells with PitStop2 and looked for this same increase in dots. This treatment almost fully blocked the appearance of dots following deciliation and completely eliminated the presence of cells with 3 or more dots (**Figure 7C-D**), suggesting a clathrin-dependent mechanism is related to these dots. Further, we wanted to know if this increase in actin dots relied on the Arp2/3 complex, so we looked for dots following deciliation in *arpc4* mutant cells (**Figure 7E**). We found that in the *arpc4* mutants dots were never observed, before or after deciliation (**Figure 7E**), suggesting these dots are dependent on not just clathrin function, but also the Arp2/3 complex.

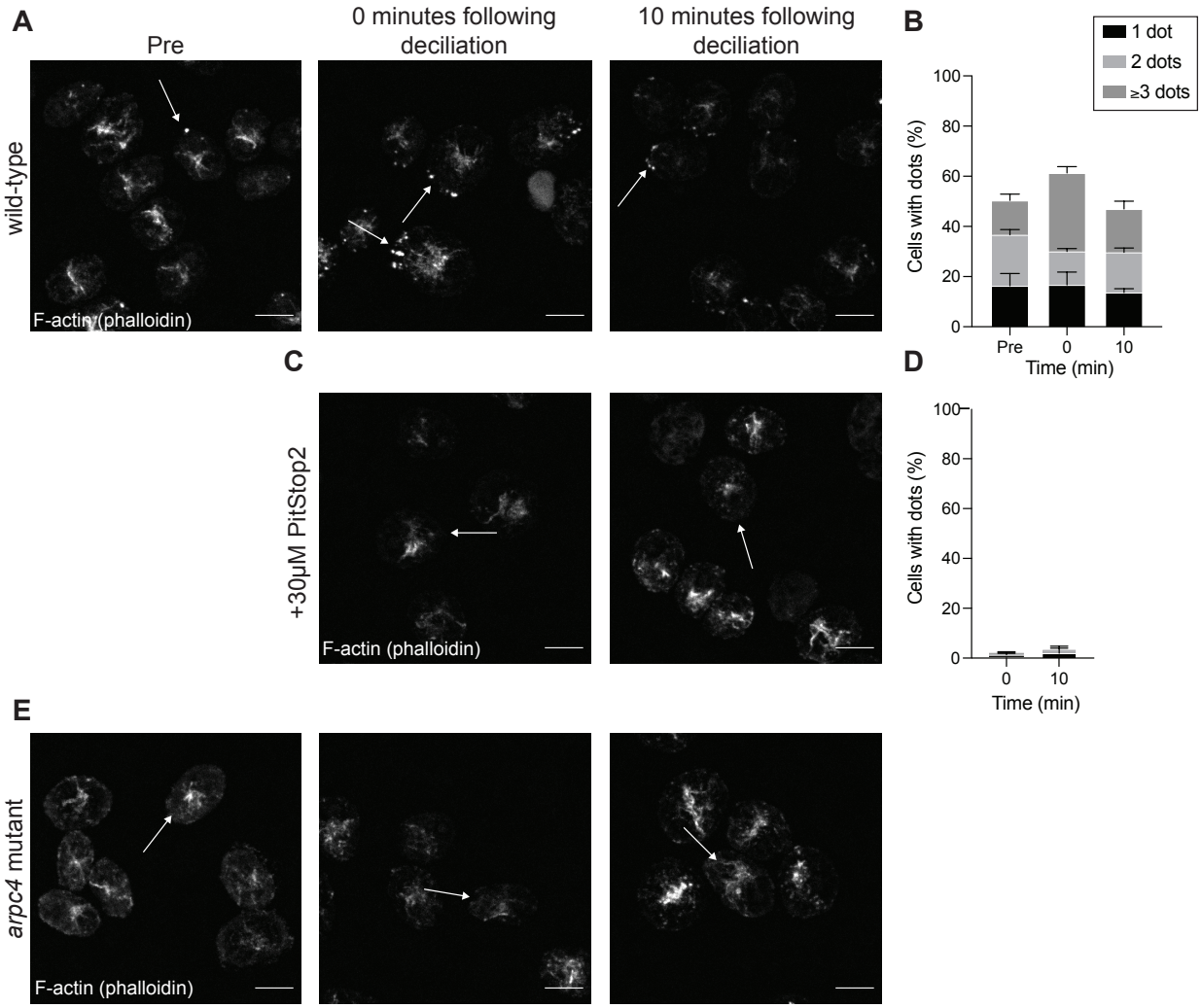

Figure 7. Actin dots are clathrin and Arp2/3 complex-dependent. A) Wild-type cells stained with phalloidin to visualize the actin network before deciliation, immediately following deciliation, and 10 minutes following deciliation. Images were taken as a z-stack using spinning disk confocal imaging and are shown as a maximum intensity projection. Scale bar represents 5μm. Arrows point to the apex of the cell. **B)** The percentage of wild-type cells with 1 dot, 2 dots, or 3 dots in Pre, 0 minute, and 10-minute samples. The bars represent the mean with error bars showing standard deviation. n=100 in 3 separate experiments. **C)** Wild-type cells treated with 30μM PitStop2 stained with phalloidin to visualize the actin immediately following deciliation and 10 minutes following deciliation. Images were taken as a z-stack using spinning disk confocal imaging and are shown as a maximum intensity projection. Scale bar represents 5μm. Arrows point to the apex of the cell. **D)** The percentage of wild-type cells treated with PitStop2 with 1 dot, 2 dot, or 3 dots in 0 minute and 10-minute samples. n=100 in 3 separate experiments. **E)** *arpc4* mutant cells stained with phalloidin before deciliation, immediately following deciliation, and 10 minutes following deciliation. Arrows point to the apex of the cells.

Clathrin localization post deciliation is altered in the absence of the Arp2/3 complex:

To directly probe the involvement of clathrin and clathrin-mediated endocytosis in ciliary assembly, we stained cells with an antibody for clathrin light chain (**Figure 8**). Wild-type cells showed an increase in clathrin signal following deciliation, perhaps due to an increase in expression (**Figure 8**). In the *arpc4* mutant cells following deciliation, we see an accumulation of clathrin in the area of the cell opposite from the cilia and the nucleus (**Figure 8, Supplemental Figure 5**). This accumulation is also observed following deciliation in wild-type or *arpc4* mutant cells treated with PitStop2 to block clathrin-mediated endocytosis (**Figure 8**), suggesting that the loss of Arp2/3 complex function and the loss of clathrin-mediated endocytosis may be linked.

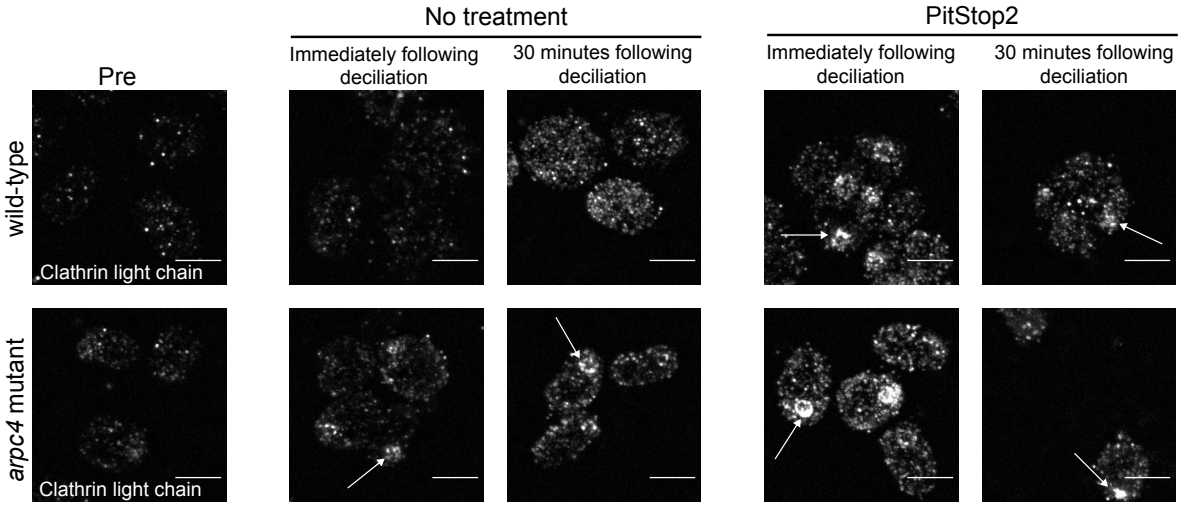

Figure 8. Clathrin is mislocalized in cells treated with PitStop2 or lacking the Arp2/3 complex. Untreated or 30μM PitStop2 treated wild-type and *arpc4* mutant cells stained with clathrin light chain antibody to visualize clathrin localization before deciliation, immediately following deciliation, and 30 minutes following deciliation. Images were taken as a z-stack using spinning disk confocal imaging and are shown as a maximum intensity projection. Arrows point to mislocalized clathrin light chain. Scale bar represents 5μm.

Ciliary membrane proteins follow different paths from the plasma membrane to the cilia:

Finally, to specifically determine if ciliary membrane and therefore membrane proteins were coming from a pool in the plasma membrane we did an experiment first described in (W. Dentler 2013). Surface proteins were biotinylated, then cells were deciliated. After the cilia regrew, they were isolated and probed for biotinylated protein (**Figure 9A**). While some proteins returned in both wild-type and *arpc4* mutant cells, some appeared to a lesser degree in *arpc4*

441 mutant cells compared to wild-type cells (**Figure 9B-E, black arrow and black bars**) and some
442 returned to a higher degree in *arpc4* mutant cells (**Figure 9B-E, grey arrow and grey bars**).
443 Other biotinylated proteins found in wild-type cilia were not found in the *arpc4* mutant cilia
444 before or after deciliation, so there is a mechanism for delivery of proteins to the cilia from the
445 plasma membrane that Arp2/3 is absolutely essential for (**Figure 9B-C**). This suggests there are
446 multiple paths to the ciliary membrane, some of which are Arp2/3 complex-independent and
447 some that are Arp2/3 complex-dependent. This may represent lateral diffusion and endocytosis
448 respectively.
449

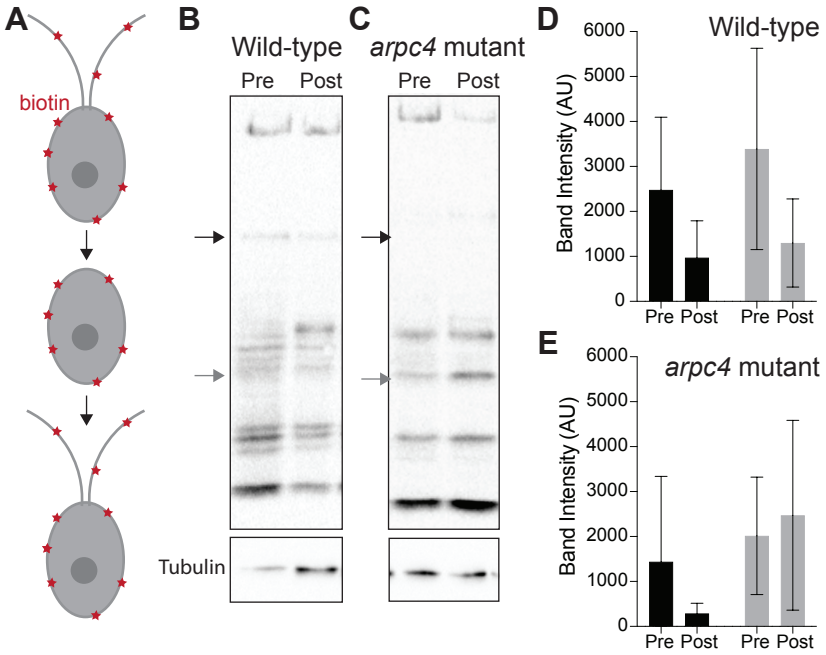

450
451
452 **Figure 9. Ciliary membrane proteins have multiple paths from the plasma membrane. A)** Cells were biotinylated,
453 deciliated, and then allowed to regrow before cilia were isolated and probed for biotinylated protein**. B)** Wild-type ciliary
454 isolate was then investigated by western blot and probed using streptavidin and tubulin as a loading control. **C)** *arpc4*
455 mutant cells ciliary isolate was investigated by western blot and probed using streptavidin. Black arrow shows ciliary
456 protein present to a higher degree in wild-type cells than the *arpc4* mutant cells. Grey arrows show ciliary protein that
457 is present to a higher degree in *arpc4* mutant cells than in wild-type cells. **D)** Bands represented by black and grey
458 arrows are quantified for the wild-type cells. Data acquired from 3 separate experiments. **E)** Bands represented by
459 black and grey arrows are quantified for the *arpc4* mutant cells. Data represented as the mean from 3 separate
460 experiments. Error bars represent standard deviation.
461
462
463
464 **DISCUSSION**
465 In this study, we investigate the Arp2/3 complex of *Chlamydomonas reinhardtii* that
466 functions to maintain and assemble cilia. This complex potentially lacks the ARPC5 subunit,
467 although it is possible that a highly divergent ARPC5 exists. In yeast, deletion of any of the
468 genes encoding Arp2/3 complex members causes severe defects and even lethality, but these
469 defects differ in severity depending on the complex members deleted, suggesting that complex
470 members have varying degrees of importance in Arp2/3 complex function (Winter, Choe, and Li
471 1999). The role of ARPC5 in actin nucleation is being investigated, but several groups have
472 found it unnecessary for overall function of the complex (Gournier et al. 2001; von Loeffelholz et
473 al. 2020). Furthermore, our data shows that knocking out function of the ARPC5-less
474 *Chlamydomonas* Arp2/3 complex genetically or chemically results in phenotypes suggesting

that the active complex functions in ciliary assembly and maintenance. Because the Arp2/3 complex has known functions in membrane dynamics, this led us to pursue models of Arp2/3 complex-dependent membrane trafficking to cilia.

Previously, three models for the trafficking of membrane proteins to cilia have been proposed (Nachury, Seeley, and Jin 2010). The first is that Golgi vesicles containing ciliary proteins are docked at the base of the cilium and fuse with the ciliary membrane inside the cilium itself. Proteins, both membrane and axonemal, have been found to be transferred from the Golgi to the cilia on or in cytoplasmic vesicles (Wood and Rosenbaum 2014). Second, Golgi vesicles containing ciliary proteins are docked near the base of the cilium still within the diffusion barrier (Papermaster, Schneider, and Besharse 1985; Nachury et al. 2007; Zuo, Guo, and Lipschutz 2009). In *Chlamydomonas*, this was first described for mastigoneme proteins, which were found to be transferred from the Golgi and then exocytosed for use on the exterior of the cell (Bouck 1971). Finally, Golgi vesicles containing proteins fuse with the plasma membrane and membrane proteins are then somehow moved across this barrier within the plasma membrane, perhaps through lateral diffusion. Evidence for this path was shown using Hedgehog signaling protein Smo, which was found to relocalize in a dynamin-independent manner from the plasma membrane to the cilia immediately after stimulation in pulse labeling studies (Milenkovic, Scott, and Rohatgi 2009).

Our data support a fourth model for the recruitment of a reservoir of membrane proteins to the cilium that is likely occurring in concert with the other models. We find the Arp2/3 complex is required for ciliary assembly, clathrin-mediated endocytosis, redistribution of ciliary proteins from the plasma membrane, and all of these activities happen immediately post-deciliation (**Figure 10A**). We hypothesize that ciliary membrane proteins and membrane targeted to the plasma membrane of the cell outside the diffusion barrier can be endocytosed and trafficked to cilia, either within or outside of the diffusion barrier in an actin and Arp2/3 complex-dependent manner.

Although our data does not eliminate the possibility of Arp2/3 complex function in supply of ciliary membrane and protein stored in other endosomal compartments, ciliary localization of proteins initially labeled on the cell surface with biotin (**Figure 9**) suggests that some ciliary membrane proteins incorporated during assembly are coming directly from the plasma membrane itself. An endocytic mechanism of trafficking in intracellular ciliogenesis has been investigated previously in mammalian RPE1 cells. The ciliary pocket found at the base of primary and motile cilia formed intracellularly has been found to be an endocytically active region (Molla-Herman et al. 2010) but clathrin mediated endocytosis was not required for ciliogenesis in those cells. The Bardet Biedl Syndrome complex (BBsome), which is involved in regulation of ciliary membrane protein composition, has been shown to interact with clathrin directly at the ciliary pocket to facilitate membrane sorting in trypanosomes (Langousis et al. 2016). Further, some BBsome complex members resemble coat proteins such as clathrin (Jin et al. 2010) suggesting a direct role for the this cilium regulatory complex in membrane budding functions. Even in *Chlamydomonas*, clathrin heavy chain has been found to localize at the base of cilia (Kaplan et al. 2012). While the mechanism was unknown, it has been shown that plasma membrane surface-exposed proteins are relocalized to cilia during ciliary regeneration (W. Dentler 2013), a result we were able to recapitulate and demonstrate depends, in part, upon the Arp2/3 complex.

Altogether, this leads us to hypothesize that the role of the Arp2/3 complex in ciliary assembly is through endocytic recruitment from a ciliary protein reservoir in the plasma membrane before newly synthesized protein and Golgi-derived membrane are capable of supplying additional materials (**Figure 10B**). While this model provides a possible route that some ciliary proteins and membranes take to the cilia, we believe this is one of several paths that can be taken to the cilia. Trafficking to cilia is likely cargo- and time-dependent, and which

path proteins take may tell us the order and speed in which they populate the cilium for subsequent function.

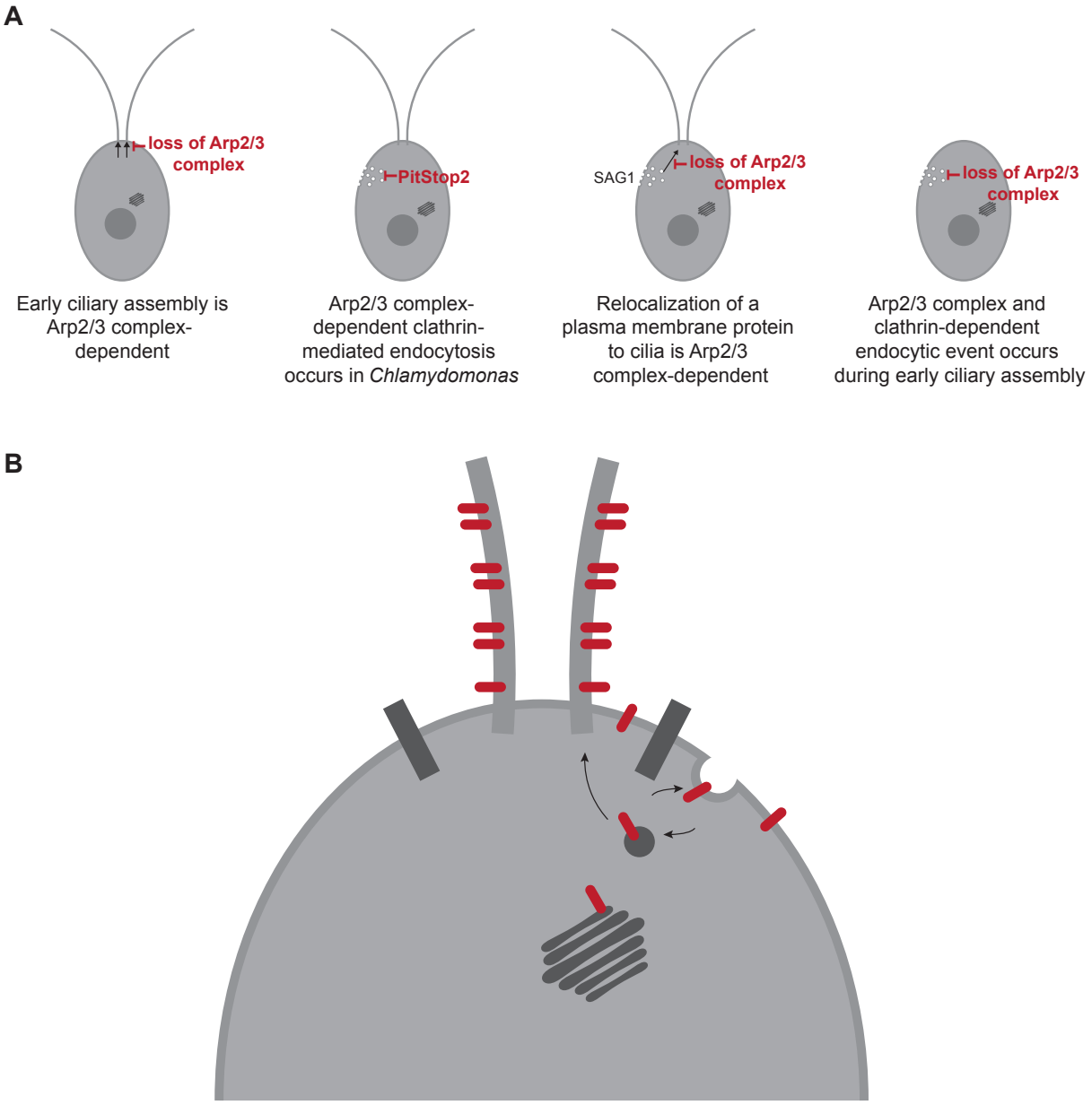

Figure 10. The Arp2/3 complex is required for membrane and protein delivery via a Golgi-independent, endocytosis-like process. A) Arp2/3-mediated actin networks are required for ciliary assembly in *Chlamydomonas* particularly during the initial stages. These actin networks are also required for clathrin-mediated endocytosis, and for the endocytosis-like relocalization of a ciliary protein from the plasma membrane to the cilia. Finally, a large endocytic event occurs immediately following deciliation that is Arp2/3 complex-mediated and dependent on clathrin-mediated endocytosis. **B)** Proposed model of membrane protein and membrane transport from the plasma membrane to the cilia through endocytosis.

METHODS

Strains:

The wild-type *Chlamydomonas* strain (CC-5325) and the *arpc4* mutant (LMJ.RY0402.232713) from the *Chlamydomonas* resource center. The *nap1* mutant was a gift from Fred Cross, Masayuki Onishi, and John Pringle. The SAG1-HA strain was a gift from William Snell. Cells were grown and maintained on 1.5% Tris-Acetate Phosphate Agar (TAP) plates (*Chlamydomonas* resource center) under constant blue (450-475 nm) and red light (625-660 nm). For experiments, cells were grown in liquid TAP media (*Chlamydomonas* resource center) overnight under constant red and blue light with agitation from a rotator. To induce gametes for mating for the SAG1-HA experiments, cells were grown in liquid M-N media (*Chlamydomonas* resource center) overnight with constant red and blue light and agitation.

Ciliary studies:

For steady state experiments, cells were treated with specified drugs [either 100μM CK-666, 250μM CK-666 (Sigma, Burlington, MA), 250μM CK-689 (Sigma, Burlington, MA), 10μM LatB (Sigma, Burlington, MA), 10μM CHX (Sigma, Burlington, MA), or 36μM BFA (Sigma, Burlington, MA)] and incubated with agitation for the allotted times. Following any incubation (as well as a pre sample), cells were diluted in an equal volume of 2% glutaraldehyde and incubated at 4º Celsius until they sediment. Following sedimentation, cells were imaged using a Zeiss DIC scope with a 40X objective. Cilia were then measured using the segmented line function in ImageJ.

For regeneration experiments, a pre sample was taken by adding cells to an equal volume of 2% glutaraldehyde. Then cells were deciliated with 115μL of 0.5N acetic acid for 45 seconds. After this short incubation, the pH was returned to normal by adding 120μL of 0.5N KOH. A 0-minute sample was again taken by adding cells to an equal volume of 2% glutaraldehyde. Then cells were incubated with agitation and allowed to regrow cilia for the allotted time period with samples taken at the indicated time points by adding cells to an equal volume of 2% glutaraldehyde. Cells in glutaraldehyde were allowed to incubate at 4º Celsius until sedimentation. Then, cells were imaged using the same Zeiss DIC scope with a 40X objective. Cilia were then measured using the segmented line function in ImageJ.

Phalloidin staining and quantification:

Procedure adapted from (Craig et al. 2019). Cells were mounted onto poly-lysine coverslips and fixed with fresh 4% paraformaldehyde in 1X HEPES. Coverslips with cells were then permeabilized with acetone and allowed to dry. Cells were rehydrated with PBS, stained with atto-phalloidin-488 (Sigma, Burlington, MA), and finally washed with PBS and allowed to dry before mounting with Fluoromount-G (Craig et al. 2019). Cells were imaged using the Nikon Spinning Disk Confocal. Z-stacks were obtained, and in ImageJ, maximum intensity projections were created for viewing.

Electron microscopy:

Cells (1mL of each strain) were deciliated via pH shock by adding 115μL of 0.5N acetic acid for 45 seconds followed by 120μL of 0.5N KOH to bring cells back to neutral pH. Cells were allowed to regrow cilia for 30 minutes. A pre sample and a 30-minute post-deciliation sample were fixed in an equal volume of 2% glutaraldehyde for 20 minutes at room temperature. Samples were then pelleted using gentle centrifugation for 10 minutes. The supernatant was removed, and cells were resuspended in 1% glutaraldehyde, 20mM sodium cacodylate. Cells were incubated for 1 hour at room temperature and then overnight at 4º Celsius. This protocol was first reported in (W. L. Dentler and Adams 1992).

590
591 *SAG1-HA Immunofluorescence:*
592 Procedure adapted from (Belzile et al. 2013). SAG1-HA cells were grown overnight in M-N
593 media to induce gametes. These cells were then treated with either 10μM LatB for 1 hour or
594 250μM CK-666 for 2 hours. Following treatment, mating was induced by adding db-cAMP
595 (ChemCruz, Santa Cruz, CA) to a final concentration of 13.5mM and incubating for 30 minutes.
596 Cells were adhered to coverslips and fixed with methanol. Cells were then dried and rehydrated
597 with PBS and incubated with 100% block (5% BSA, 1% fish gelatin) for 30 minutes. The 100%
598 block was replaced with new 100% block containing 10% normal goat serum for another 30-
599 minute incubation. The primary antibody (rat anti-HA, Sigma, Burlington, MA) was diluted
600 1:1000 in 20% block in PBS. Coverslips were incubated at 4º Celsius in a humidified chamber
601 overnight. The primary antibody was removed and washed away with 3 10-minute PBS washes.
602 The secondary (anti-rat IgG-Alexafluor 488, Invitrogen, Carlsbad, CA) was added and coverslips
603 were incubated at room temperature for 1 hour. This was followed by 3 more 10-minute PBS
604 washes and finally mounting with Fluoromount-G. Cells were imaged using a Nikon widefield
605 microscope. Z-stacks were obtained, and maximum intensity projections were created for
606 visualization and sum slices were created for quantification using ImageJ.
607
608 Images were quantified by using line scans from the apex of the cells to the basal region of the
609 cells farthest away from the apex. Line scans were then normalized, and background subtracted
610 before being combined into single graphs. Using the line scans, the intensity of signal at the
611 basal region of the cells was subtracted from the signal at the apical region. Finally, cells with a
612 difference over 30 were considered to be apically enriched and this was quantified as
613 percentage of cells with apical staining.
614
615 *SAG1-HA western blot:*
616 Procedure adapted from (Belzile et al. 2013). SAG1-HA cells were grown overnight in M-N
617 media to induce gametes. These cells were then treated with either 10μM LatB for 1 hour or
618 250μM CK-666 for 2 hours. Following treatment, mating induction was done by adding db-cAMP
619 to a final concentration of 13.5mM and incubating for 10 minutes. Cells were then treated with
620 0.01% trypsin for 5 minutes, pelleted (at 500xg for 2 minutes), resuspended in lysis buffer (5%
621 glycerol, 1% NP-40, 1mM DTT, 1X protease inhibitors), and then lysed with bead beating. Cell
622 debris was spun down at 14000xg for 15 minutes. An equal amount of protein was loaded to a
623 10% SDS-PAGE gel. The resulting gel was transferred to membrane which was then blocked
624 with 5% milk in PBST. The primary antibody (rabbit anti-HA, Cell Signaling, Danvers, MA)
625 diluted to 1:1000 in 1% BSA, 1% milk was added and incubated overnight at 4º Celsius. Primary
626 antibody washed off with 3 10-minute PBST washes. Secondary antibody (anti rabbit IgG,
627 Invitrogen, Carlsbad, CA) was diluted to 1:5000 in 1% milk. 1% BSA was added, and the blot
628 was incubated for 1 hour. Membrane was probed with West Pico Chemiluminescent Pico
629 Substrate (Invitrogen, Carlsbad, CA). Total protein was determined with amido black staining.
630 Band intensity was measured in ImageJ and normalized to total protein
631
632 *Membrane stain:*
633 FM 4-64FX membrane stain (Thermo, Waltham, MA) was diluted to a stock concentration of
634 200μg/mL. Cells were adhered to poly-lysine coverslips. After a 5-minute incubation, cells were
635 tilted off and 5μg/mL of ice-cold stain in Hank's Buffered Salt Solution (HBSS) without
636 magnesium or calcium was added for 1 minute. The stain was tilted off and cells were fixed with
637 ice cold 4% paraformaldehyde in HBSS without magnesium or calcium for 15 minutes.
638 Coverslips were then rinsed 3 times for 10 minutes each in ice cold HBSS without magnesium
639 or calcium. Finally, cells were mounted with Fluoromount-G and imaged using the Nikon

640 Spinning Disk Confocal. Z-stacks were taken and combined into sum projections using ImageJ.
641 The background corrected total cell fluorescence was then calculated by taking the integrated
642 density and subtracting the sum of the area and the mean background intensity.
643
644 *Clathrin light chain immunofluorescence:*
645 Cells were grown overnight in TAP media. Cells were deciliated using low pH shock. Cells are
646 then adhered to coverslips and fixed with 4% PFA in 1X HEPES. Cells were then dried and
647 rehydrated with PBS and incubated with 100% block (5% BSA, 1% fish gelatin) for 1 hour. The
648 primary antibody (goat anti-clathrin light chain, Abcam, Cambridge, UK or rabbit anti-acetylated
649 tubulin, Cell Signaling, Danvers, MA) was diluted 1:1000 in 20% block in PBS. Coverslips were
650 incubated at 4º Celsius in a humidified chamber overnight. The primary antibody was removed
651 and washed away with 3 10-minute PBS washes. The secondary (donkey anti-goat IgG-
652 Alexafluor 488, Invitrogen, Carlsbad, CA or goat anti-rabbit IgG-Alexafluor 568, Invitrogen,
653 Carlsbad, CA) was added and coverslips were incubated at room temperature for 1 hour. For
654 cells stained with DAPI, DAPI (Biotium, Fremont, CA) was added for the last 10 minutes of
655 secondary antibody incubation. This was followed by 3 more 10-minute PBS washes and finally
656 mounting with Fluoromount-G. Cells were imaged using a Nikon widefield microscope. Z-stacks
657 were obtained, and maximum intensity projections were created for visualization and sum slices
658 were created for quantification using ImageJ.
659
660 *Biotin ciliary isolation:*
661 Procedure adapted from (W. Dentler 2013). 100mL of cells were grown in TAP for each
662 condition until they reached an OD_{730} of 1.6 or above. Cells were then spun down and
663 resuspended in M1 media and allowed to grow overnight. The next day cells were spun down at
664 1800rpm for 3 minutes and resuspended in HM Media (10mM HEPES, 5mM MgSO4, pH 7.2).
665 Solid biotin (Thermo, Waltham, MA) was added to 20µg/mL for each strain and incubated for 5
666 minutes with agitation. Cells were diluted with 10 volumes of fresh M1 media before being spun
667 down at 1800rpm for 3 minutes. After all cells were pelleted, they were washed with fresh M1
668 media three times. A pre sample was set aside (100mL) and the remainder of the cells were
669 resuspended in 4.5 pH M1 media for 45 seconds before being spun down again at 1800rpm for
670 3 minutes. Cells were then resuspended in pH 7.0 media and allowed to regrow their cilia for 4
671 hours. A sample was taken pre-biotinylation to use as a control for non-specific streptavidin
672 binding.
673
674 Meanwhile, the cilia were isolated from the pre sample. The samples were centrifuged for 3
675 minutes at 1800rpm. Supernatant was drained and each pellet was resuspended in 2 mL of
676 10mM HEPES (pH 7.4). This was repeated 2 times. Then each pellet was resuspended in 1 mL
677 of fresh ice-cold 4% HMDS (10mM HEPES pH 7.4, 5mM MgSO4, 1mM DTT, 4% w/v sucrose).
678 Cells were deciliated by incubating with 25mM dibucaine for 2 minutes. Then ice cold HMDS
679 with 0.5mM EGTA was added (1mL per 1.5mL of cells). This was then centrifuged for 3 minutes
680 at 1800rpm. Supernatant was collected for each sample. Then HMDS with 25% sucrose was
681 layered beneath the supernatant (2 mL of 25% HMDS for 1mL of supernatant) to create an
682 interface. This was centrifuged at 4º Celsius for 10 min at 2400rpm with no brake to avoid
683 disrupting interface where cilia should now be located. Cilia were removed, pelleted at 21130xg
684 for 30 minutes, then resuspended in lysis buffer (5% glycerol, 1% NP-40, 1mM DTT, 1X
685 protease inhibitors). This was repeated with the post samples 4 hours following deciliation. An
686 equal amount of protein was loaded to a 10% SDS-PAGE gel. The resulting gel was transferred
687 to membrane. The membrane was washed 2x with PBSAT (PBST + 0.1% BSA), then incubated
688 with HRP-conjugated streptavidin (Thermo, Waltham, MA) for 1 hour. The membrane was then
689 washed 3 times with PBSAT (10 minutes each) and 3 times with PBST (15 minutes each).

Membrane was probed with West Pico Chemiluminescent Pico Substrate (Invitrogen, Carlsbad, CA).

Homology modeling and sequence studies:
Arp2/3 homology model was created using the Modeller plugin in UCSF Chimera. The template used was 1U2Z (Nolen, Littlefield, and Pollard 2004; Sali and Blundell 1993; Pettersen et al. 2004). Percent identity and similarity is calculated in relation to the human Arp2/3 complex members using a MUSCLE alignment in Geneious. The homology model was visualized and conservation was mapped on the protein surface using Chimera (Pettersen et al. 2004).

Statistical analysis:
Statistical analyses were done if GraphPad Prism Version 9. For any experiments comparing 2 groups (**Figure 1B, 3D, 4C, 5C, and 5E**) an unpaired student's t-test was used to determine P value. For experiments comparing multiple samples at a single time point (**Figure 1A and 2B**), an ANOVA was used. Finally, for any graphs covering several time points (**Figure 1C, 1D, 2C, 3B, and 6E),** multiple comparisons were performed (Tukey's and Sidak's). For all experiments **** P<0.0001, *** P<0.001, ** P<0.01, * P<0.1.

ACKNOWLEDGEMENTS:

Our most sincere gratitude to William Dentler for providing his expertise especially in looking at the electron microscopy images and for his helpful advice, William Snell for generously providing the SAG1-HA strain, Masayuki Onishi for generously providing the *nap1* mutant strain, Henry Higgs for his feedback on the manuscript, Ann Lavanway for assistance with microscopy, and the Avasthi lab for all their help throughout the project. We would also like to thank David Sept and Courtney M Schroeder for the help with the original version of this paper and for providing helpful comments throughout the process.

We also thank our funding sources including the Madison and Lila Self Graduate Fellowship at the University of Kansas Medical Center and the MIRA (R35GM128702). Finally, we thank the BioMT core at Dartmouth College (NIH/NIGMS COBRE award P20-GM113132), the Genomics and Molecular Biology Shared Resources Core (NCI Cancer Center Support Grant 5P30CA023108-37), and the KIDDRC NIH U54 HD 090216 at the University of Kansas Medical Center, Kansas City, KS 66160.

REFERENCES:

Adams, A E, and J R Pringle. 1984. "Relationship of Actin and Tubulin Distribution to Bud Growth in Wild-Type and Morphogenetic-Mutant Saccharomyces Cerevisiae." *Journal of Cell Biology* 98 (3): 934–45. https://doi.org/10.1083/jcb.98.3.934.

Aghamohammadzadeh, Soheil, and Kathryn R. Ayscough. 2009. "Differential Requirements for Actin during Yeast and Mammalian Endocytosis." *Nature Cell Biology* 11 (8): 1039–42. https://doi.org/10.1038/ncb1918.

Avasthi, Prachee, Masayuki Onishi, Joel Karpiak, Ryosuke Yamamoto, Luke Mackinder, Martin C Jonikas, Winfield S Sale, Brian Shoichet, John R Pringle, and Wallace F Marshall. 2014. "Actin Is Required for IFT Regulation in Chlamydomonas Reinhardtii." *Current Biology* 24 (17): 2025–32. https://doi.org/10.1016/j.cub.2014.07.038.

Ayscough, K. R., J. Stryker, N. Pokala, M. Sanders, P. Crews, and D. G. Drubin. 1997. "High Rates of Actin Filament Turnover in Budding Yeast and Roles for Actin in Establishment and

739 Maintenance of Cell Polarity Revealed Using the Actin Inhibitor Latrunculin-A." *The*
740 *Journal of Cell Biology* 137 (2): 399–416. https://doi.org/10.1083/jcb.137.2.399.
741 Basu, Roshni, Emilia Laura Munteanu, and Fred Chang. 2014. "Role of Turgor Pressure in
742 Endocytosis in Fission Yeast." *Molecular Biology of the Cell* 25 (5): 679–87.
743 https://doi.org/10.1091/mbc.E13-10-0618.
744 Belzile, Olivier, Carmen I Hernandez-Lara, Qian Wang, and William J Snell. 2013. "Regulated
745 Membrane Protein Entry into Flagella Is Facilitated by Cytoplasmic Microtubules and
746 Does Not Require IFT." *Current Biology : CB* 23 (15): 1460–65.
747 https://doi.org/10.1016/j.cub.2013.06.025.
748 Bouck, G. Benjamin. 1971. "THE STRUCTURE, ORIGIN, ISOLATION, AND COMPOSITION OF THE
749 TUBULAR MASTIGONEMES OF THE OCHROMONAS FLAGELLUM." *Journal of Cell Biology*
750 50 (2): 362–84. https://doi.org/10.1083/jcb.50.2.362.
751 Campellone, K., and M. Welch. 2010. "A Nucleator Arms Race: Cellular Control of Actin
752 Assembly." *Nature Reviews Molecular Cell Biology* 11: 237–51.
753 Carlsson, Anders E., and Philip V. Bayly. 2014. "Force Generation by Endocytic Actin Patches in
754 Budding Yeast." *Biophysical Journal* 106 (8): 1596–1606.
755 https://doi.org/10.1016/j.bpj.2014.02.035.
756 Cheng, Xi, Gai Liu, Wenting Ke, Lijuan Zhao, Bo Lv, Xiaocui Ma, Nannan Xu, et al. 2017. "Building
757 a Multipurpose Insertional Mutant Library for Forward and Reverse Genetics in
758 Chlamydomonas." *Plant Methods* 13 (1): 36. https://doi.org/10.1186/s13007-017-0183-
759 5.
760 Craig, Evan W., David M. Mueller, Brae M. Bigge, Miroslava Schaffer, Benjamin D. Engel, and
761 Prachee Avasthi. 2019. "The Elusive Actin Cytoskeleton of a Green Alga Expressing Both
762 Conventional and Divergent Actins." *Molecular Biology of the Cell*, mbc.E19-03-0141.
763 https://doi.org/10.1091/mbc.E19-03-0141.
764 Dentler, W L, and C Adams. 1992. "Flagellar Microtubule Dynamics in Chlamydomonas:
765 Cytochalasin D Induces Periods of Microtubule Shortening and Elongation; and
766 Colchicine Induces Disassembly of the Distal, but Not Proximal, Half of the Flagellum."
767 *The Journal of Cell Biology* 117 (6): 1289–98. https://doi.org/10.1083/jcb.117.6.1289.
768 Dentler, William. 2013. "A Role for the Membrane in Regulating Chlamydomonas Flagellar
769 Length." *PLOS ONE* 8 (1): e53366. https://doi.org/10.1371/journal.pone.0053366.
770 Diener, Dennis R, Pietro Lupetti, and Joel L Rosenbaum. 2015. "Proteomic Analysis of Isolated
771 Ciliary Transition Zones Reveals the Presence of ESCRT Proteins." *Current Biology : CB* 25
772 (3): 379–84. https://doi.org/10.1016/j.cub.2014.11.066.
773 Farina, Francesca, Jérémie Gaillard, Christophe Guérin, Yohann Couté, James Sillibourne,
774 Laurent Blanchoin, and Manuel Théry. 2016. "The Centrosome Is an Actin-Organizing
775 Centre." *Nature Cell Biology* 18 (1): 65–75. https://doi.org/10.1038/ncb3285.
776 Goode, Bruce L, Julian A Eskin, and Beverly Wendland. 2015. "Actin and Endocytosis in Budding
777 Yeast." *Genetics* 199 (2): 315–58. https://doi.org/10.1534/genetics.112.145540.
778 Gournier, Helene, Erin D. Goley, Hanspeter Niederstrasser, Thong Trinh, and Matthew D.
779 Welch. 2001. "Reconstitution of Human Arp2/3 Complex Reveals Critical Roles of
780 Individual Subunits in Complex Structure and Activity." *Molecular Cell* 8 (5): 1041–52.
781 https://doi.org/10.1016/S1097-2765(01)00393-8.

782 Hetrick, Byron, Min Suk Han, Luke A Helgeson, and Brad J Nolen. 2013. "Small Molecules CK-666
783 and CK-869 Inhibit Actin-Related Protein 2/3 Complex by Blocking an Activating
784 Conformational Change." *Chemistry & Biology* 20 (5): 701–12.
785 https://doi.org/10.1016/j.chembiol.2013.03.019.
786 Hirono, Masafumi, Satomi Uryu, Akio Ohara, Takako Kato-Minoura, and Ritsu Kamiya. 2003.
787 "Expression of Conventional and Unconventional Actins in Chlamydomonas Reinhardtii
788 upon Deflagellation and Sexual Adhesion." *Eukaryotic Cell* 2 (3): 486–93.
789 https://doi.org/10.1128/ec.2.3.486-493.2003.
790 Huang, Kaiyao, Dennis R. Diener, Aaron Mitchell, Gregory J. Pazour, George B. Witman, and Joel
791 L. Rosenbaum. 2007. "Function and Dynamics of PKD2 in Chlamydomonas Reinhardtii
792 Flagella." *Journal of Cell Biology* 179 (3): 501–14.
793 https://doi.org/10.1083/jcb.200704069.
794 Hunnicutt, G. R., M. G. Kosfiszer, and W. J. Snell. 1990. "Cell Body and Flagellar Agglutinins in
795 Chlamydomonas Reinhardtii: The Cell Body Plasma Membrane Is a Reservoir for
796 Agglutinins Whose Migration to the Flagella Is Regulated by a Functional Barrier." *The*
797 *Journal of Cell Biology* 111 (4): 1605–16. https://doi.org/10.1083/jcb.111.4.1605.
798 Inoue, Daisuke, Dorian Obino, Judith Pineau, Francesca Farina, Jérémie Gaillard, Christophe
799 Guerin, Laurent Blanchoin, Ana-Maria Lennon-Duménil, and Manuel Théry. 2019. "Actin
800 Filaments Regulate Microtubule Growth at the Centrosome." *The EMBO Journal* 38 (11).
801 https://doi.org/10.15252/embj.201899630.
802 Jack, Brittany, David M. Mueller, Ann C. Fee, Ashley L. Tetlow, and Prachee Avasthi. 2019.
803 "Partially Redundant Actin Genes in Chlamydomonas Control Transition Zone
804 Organization and Flagellum-Directed Traffic." *Cell Reports* 27 (8): 2459-2467.e3.
805 https://doi.org/10.1016/j.celrep.2019.04.087.
806 Jin, Hua, Susan Roehl White, Toshinobu Shida, Stefan Schulz, Mike Aguiar, Steven P. Gygi, J.
807 Fernando Bazan, and Maxence V. Nachury. 2010. "The Conserved Bardet-Biedl
808 Syndrome Proteins Assemble a Coat That Traffics Membrane Proteins to Cilia." *Cell* 141
809 (7): 1208–19. https://doi.org/10.1016/j.cell.2010.05.015.
810 Kaplan, Oktay I., David B. Doroquez, Sebiha Cevik, Rachel V. Bowie, Lara Clarke, Anna A.W.M.
811 Sanders, Katarzyna Kida, Joshua Z. Rappoport, Piali Sengupta, and Oliver E. Blacque.
812 2012. "Endocytosis Genes Facilitate Protein and Membrane Transport in C. Elegans
813 Sensory Cilia." *Current Biology* 22 (6): 451–60.
814 https://doi.org/10.1016/j.cub.2012.01.060.
815 Kato-Minoura, T, S Uryu, M Hirono, and R Kamiya. 1998. "Highly Divergent Actin Expressed in a
816 Chlamydomonas Mutant Lacking the Conventional Actin Gene." *Biochemical and*
817 *Biophysical Research Communications* 251 (1): 71–76.
818 https://doi.org/10.1006/bbrc.1998.9373.
819 Kiesel, Petra, Gonzalo Alvarez Viar, Nikolai Tsoy, Riccardo Maraspini, Peter Gorilak, Vladimir
820 Varga, Alf Honigmann, and Gaia Pigino. 2020. "The Molecular Structure of Mammalian
821 Primary Cilia Revealed by Cryo-Electron Tomography." *Nature Structural & Molecular*
822 *Biology*, September. https://doi.org/10.1038/s41594-020-0507-4.
823 Kim, Joon, Ji Eun Lee, Susanne Heynen-Genel, Eigo Suyama, Keiichiro Ono, Kiyoung Lee, Trey
824 Ideker, Pedro Aza-Blanc, and Joseph G. Gleeson. 2010. "Functional Genomic Screen for

825 Modulators of Ciliogenesis and Cilium Length." *Nature* 464 (7291): 1048–51.
826 https://doi.org/10.1038/nature08895.
827 Langousis, Gerasimos, Michelle M. Shimogawa, Edwin A. Saada, Ajay A. Vashisht, Roberto
828 Spreafico, Andrew R. Nager, William D. Barshop, Maxence V. Nachury, James A.
829 Wohlschlegel, and Kent L. Hill. 2016. "Loss of the BBSome Perturbs Endocytic Trafficking
830 and Disrupts Virulence of Trypanosoma Brucei." *Proceedings of the National Academy*
831 *of Sciences of the United States of America* 113 (3): 632–37.
832 https://doi.org/10.1073/pnas.1518079113.
833 Lefebvre, P. A., S. A. Nordstrom, J. E. Moulder, and J. L. Rosenbaum. 1978. "Flagellar Elongation
834 and Shortening in Chlamydomonas. IV. Effects of Flagellar Detachment, Regeneration,
835 and Resorption on the Induction of Flagellar Protein Synthesis." *The Journal of Cell*
836 *Biology* 78 (1): 8–27. https://doi.org/10.1083/jcb.78.1.8.
837 Lefebvre, Paul A. 1995. "Flagellar Amputation and Regeneration in Chlamydomonas." In
838 *Methods in Cell Biology*, 47:3–7. Elsevier.
839 Li, Xiaobo, Weronika Patena, Friedrich Fauser, Robert E. Jinkerson, Shai Saroussi, Moritz T.
840 Meyer, Nina Ivanova, et al. 2019. "A Genome-Wide Algal Mutant Library and Functional
841 Screen Identifies Genes Required for Eukaryotic Photosynthesis." *Nature Genetics* 51
842 (4): 627–35. https://doi.org/10.1038/s41588-019-0370-6.
843 Loeffelholz, Ottilie von, Andrew Purkiss, Luyan Cao, Svend Kjaer, Naoko Kogata, Guillaume
844 Romet-Lemonne, Michael Way, and Carolyn A. Moores. 2020. "Cryo-EM of Human
845 Arp2/3 Complexes Provides Structural Insights into Actin Nucleation Modulation by
846 ARPC5 Isoforms." *BioRxiv*, January, 2020.05.01.071704.
847 https://doi.org/10.1101/2020.05.01.071704.
848 Marszalek, Joseph R, Xinran Liu, Elizabeth A Roberts, Daniel Chui, Jamey D Marth, David S
849 Williams, and Lawrence S.B Goldstein. 2000. "Genetic Evidence for Selective Transport
850 of Opsin and Arrestin by Kinesin-II in Mammalian Photoreceptors." *Cell* 102 (2): 175–87.
851 https://doi.org/10.1016/S0092-8674(00)00023-4.
852 Milenkovic, Ljiljana, Matthew P. Scott, and Rajat Rohatgi. 2009. "Lateral Transport of
853 Smoothened from the Plasma Membrane to the Membrane of the Cilium." *The Journal*
854 *of Cell Biology* 187 (3): 365–74. https://doi.org/10.1083/jcb.200907126.
855 Molla-Herman, Anahi, Rania Ghossoub, Thierry Blisnick, Alice Meunier, Catherine Serres, Flora
856 Silbermann, Chris Emmerson, et al. 2010. "The Ciliary Pocket: An Endocytic Membrane
857 Domain at the Base of Primary and Motile Cilia." *Journal of Cell Science* 123 (Pt 10):
858 1785–95. https://doi.org/10.1242/jcs.059519.
859 Nachury, Maxence V., Alexander V. Loktev, Qihong Zhang, Christopher J. Westlake, Johan
860 Peränen, Andreas Merdes, Diane C. Slusarski, et al. 2007. "A Core Complex of BBS
861 Proteins Cooperates with the GTPase Rab8 to Promote Ciliary Membrane Biogenesis."
862 *Cell* 129 (6): 1201–13. https://doi.org/10.1016/j.cell.2007.03.053.
863 Nachury, Maxence V., E. Scott Seeley, and Hua Jin. 2010. "Trafficking to the Ciliary Membrane:
864 How to Get across the Periciliary Diffusion Barrier?" *Annual Review of Cell and*
865 *Developmental Biology* 26: 59–87.
866 https://doi.org/10.1146/annurev.cellbio.042308.113337.
867 Nolen, Brad J., Ryan S. Littlefield, and Thomas D. Pollard. 2004. "Crystal Structures of Actin-
868 Related Protein 2/3 Complex with Bound ATP or ADP." *Proceedings of the National*

869 *Academy of Sciences of the United States of America* 101 (44): 15627.
870 https://doi.org/10.1073/pnas.0407149101.
871 Onishi, M., K. Pecani, T. th Jones, J. R. Pringle, and F. R. Cross. 2018. "F-Actin Homeostasis
872 through Transcriptional Regulation and Proteasome-Mediated Proteolysis." *Proc Natl*
873 *Acad Sci U S A* 115 (28): E6487-e6496. https://doi.org/10.1073/pnas.1721935115.
874 Onishi, M., J. R. Pringle, and F. R. Cross. 2016. "Evidence That an Unconventional Actin Can
875 Provide Essential F-Actin Function and That a Surveillance System Monitors F-Actin
876 Integrity in Chlamydomonas." *Genetics* 202 (3): 977–96.
877 https://doi.org/10.1534/genetics.115.184663.
878 Onishi, Masayuki, James G. Umen, Frederick R. Cross, and John R. Pringle. 2019. "Cleavage-
879 Furrow Formation without F-Actin in Chlamydomonas</Em>." *BioRxiv*, January,
880 789016. https://doi.org/10.1101/789016.
881 Papermaster, D. S., B. G. Schneider, and J. C. Besharse. 1985. "Vesicular Transport of Newly
882 Synthesized Opsin from the Golgi Apparatus toward the Rod Outer Segment.
883 Ultrastructural Immunocytochemical and Autoradiographic Evidence in Xenopus
884 Retinas." *Investigative Ophthalmology & Visual Science* 26 (10): 1386–1404.
885 Park, Tae Joo, Brian J. Mitchell, Philip B. Abitua, Chris Kintner, and John B. Wallingford. 2008.
886 "Dishevelled Controls Apical Docking and Planar Polarization of Basal Bodies in Ciliated
887 Epithelial Cells." *Nature Genetics* 40 (7): 871–79. https://doi.org/10.1038/ng.104.
888 Pasquale, S M, and U W Goodenough. 1987. "Cyclic AMP Functions as a Primary Sexual Signal in
889 Gametes of Chlamydomonas Reinhardtii." *The Journal of Cell Biology* 105 (5): 2279–92.
890 https://doi.org/10.1083/jcb.105.5.2279.
891 Pazour, Gregory J., Sheila A. Baker, James A. Deane, Douglas G. Cole, Bethany L. Dickert, Joel L.
892 Rosenbaum, George B. Witman, and Joseph C. Besharse. 2002. "The Intraflagellar
893 Transport Protein, IFT88, Is Essential for Vertebrate Photoreceptor Assembly and
894 Maintenance." *Journal of Cell Biology* 157 (1): 103–14.
895 https://doi.org/10.1083/jcb.200107108.
896 Pedersen, Lotte B., and Joel L. Rosenbaum. 2008. "Intraflagellar Transport (IFT) Role in Ciliary
897 Assembly, Resorption and Signalling." *Current Topics in Developmental Biology* 85: 23–
898 61. https://doi.org/10.1016/S0070-2153(08)00802-8.
899 Pettersen, Eric F., Thomas D. Goddard, Conrad C. Huang, Gregory S. Couch, Daniel M.
900 Greenblatt, Elaine C. Meng, and Thomas E. Ferrin. 2004. "UCSF Chimera--a Visualization
901 System for Exploratory Research and Analysis." *Journal of Computational Chemistry* 25
902 (13): 1605–12. https://doi.org/10.1002/jcc.20084.
903 Robinson, Robert C., Kirsi Turbedsky, Donald A. Kaiser, Jean-Baptiste Marchand, Henry N. Higgs,
904 Senyon Choe, and Thomas D. Pollard. 2001. "Crystal Structure of Arp2/3 Complex."
905 *Science* 294 (5547): 1679. https://doi.org/10.1126/science.1066333.
906 Rohatgi, Rajat, and William J Snell. 2010. "The Ciliary Membrane." *Current Opinion in Cell*
907 *Biology* 22 (4): 541–46. https://doi.org/10.1016/j.ceb.2010.03.010.
908 Rosenbaum, J. L., J. E. Moulder, and D. L. Ringo. 1969. "Flagellar Elongation and Shortening in
909 Chlamydomonas. The Use of Cycloheximide and Colchicine to Study the Synthesis and
910 Assembly of Flagellar Proteins." *The Journal of Cell Biology* 41 (2): 600–619.
911 https://doi.org/10.1083/jcb.41.2.600.

912 Saito, Masaki, Wataru Otsu, Kuo-Shun Hsu, Jen-Zen Chuang, Teruyuki Yanagisawa, Vincent
913 Shieh, Taku Kaitsuka, Fan-Yan Wei, Kazuhito Tomizawa, and Ching-Hwa Sung. 2017.
914 "Tctex-1 Controls Ciliary Resorption by Regulating Branched Actin Polymerization and
915 Endocytosis." *EMBO Reports* 18 (8): 1460–72.
916 https://doi.org/10.15252/embr.201744204.
917 Sali, A., and T. L. Blundell. 1993. "Comparative Protein Modelling by Satisfaction of Spatial
918 Restraints." *Journal of Molecular Biology* 234 (3): 779–815.
919 https://doi.org/10.1006/jmbi.1993.1626.
920 Spector, Ilan, Nava R. Shochet, Dina Blasberger, and Yoel Kashman. 1989. "Latrunculins—Novel
921 Marine Macrolides That Disrupt Microfilament Organization and Affect Cell Growth: I.
922 Comparison with Cytochalasin D." *Cell Motility* 13 (3): 127–44.
923 https://doi.org/10.1002/cm.970130302.
924 Wingfield, Jenna L, Ilaria Mengoni, Heather Bomberger, Yu-Yang Jiang, Jonathon D Walsh, Jason
925 M Brown, Tyler Picariello, et al. 2017. "IFT Trains in Different Stages of Assembly Queue
926 at the Ciliary Base for Consecutive Release into the Cilium." Edited by Erwin J G
927 Peterman. *ELife* 6 (May): e26609. https://doi.org/10.7554/eLife.26609.
928 Winter, D. C., E. Y. Choe, and R. Li. 1999. "Genetic Dissection of the Budding Yeast Arp2/3
929 Complex: A Comparison of the in Vivo and Structural Roles of Individual Subunits."
930 *Proceedings of the National Academy of Sciences of the United States of America* 96
931 (13): 7288–93. https://doi.org/10.1073/pnas.96.13.7288.
932 Wood, Christopher R., and Joel L. Rosenbaum. 2014. "Proteins of the Ciliary Axoneme Are
933 Found on Cytoplasmic Membrane Vesicles during Growth of Cilia." *Current Biology* 24
934 (10): 1114–20. https://doi.org/10.1016/j.cub.2014.03.047.
935 Wu, Chien-Ting, Hsin-Yi Chen, and Tang K. Tang. 2018. "Myosin-Va Is Required for Preciliary
936 Vesicle Transportation to the Mother Centriole during Ciliogenesis." *Nature Cell Biology*
937 20 (2): 175–85. https://doi.org/10.1038/s41556-017-0018-7.
938 Zuo, Xiaofeng, Wei Guo, and Joshua H. Lipschutz. 2009. "The Exocyst Protein Sec10 Is Necessary
939 for Primary Ciliogenesis and Cystogenesis In Vitro." *Molecular Biology of the Cell* 20 (10):
940 2522–29. https://doi.org/10.1091/mbc.e08-07-0772.
941